Heteronuclear and Homonuclear High-Spin Alkali Trimers on Helium Nanodroplets

Johann Nagl, Gerald Auböck, Andreas W. Hauser, Olivier Allard, Carlo Callegari, and Wolfgang E. Ernst*

Institute of Experimental Physics, TU Graz, Petersgasse 16, A-8010 Graz, Austria, EU

(Received 27 August 2007; published 13 February 2008)

The electronic excitation spectra of all possible homo- and heteronuclear high-spin (quartet) trimers of K and Rb (K_xRb_{3-x}, $x = 0 \ldots 3$) assembled on the surface of superfluid helium droplets, are measured in the spectral range from 10 600 to 17 400 cm^{-1}. A regular series of corresponding bands is observed, reflecting the similar electronic structure of all these trimers. For the assignment and separation of overlapping bands, we determine x directly, with mass-selected beam depletion, and indirectly with a V-type double-resonance scheme. The assignment is confirmed by high-level *ab initio* calculations of the electronic structure of the bare trimers. The level structure is rationalized in terms of harmonic-oscillator states of the three valence electrons in a quantum-dot-like confining potential. We predict that three should be a magic number for high-spin alkali clusters.

DOI: 10.1103/PhysRevLett.100.063001 PACS numbers: 33.20.Kf, 31.15.A−, 42.62.Fi, 67.25.dw

Helium nanodroplet isolation spectroscopy has become a powerful tool for the production and probing of molecules, clusters, and chemical reactions at low temperatures [1]. Dopant species are cooled down to the internal temperature of the droplet (0.37 K [2]) and readily form complexes, weakly bound ones being favored [3]. Among all dopants, alkali atoms are unique in that they remain on the surface [4,5] rather than becoming solvated inside the droplet; because of the different formation energy, high-spin molecules are almost exclusively observed, instead of the expected statistical mixture [3,6].

High-spin (quartet) alkali trimers were immediately recognized as a model system to investigate van der Waals forces between constituents with highly deformable outer electron shells [6]. Soon, the importance of three-body forces was shown [7,8]; in this description one has chosen to view valence electrons as bound each to its own atom. In large metal clusters, one describes them as delocalized within a confining potential, thus emphasizing the electronic structure over the geometric structure. This leads to a shell model, which is of great interest in the study of the electronic structure and excitation of metal clusters and quantum dots, particularly as perturbed by a magnetic field [9].

The explosive growth of Bose-Einstein condensation research [10,11], largely based on spin-polarized diluted gases of alkali atoms, has made such topics as two- and three-body collisions [12,13], molecule formation, especially by magnetic tuning of Feshbach resonances [14,15], and Efimov states [16,17], of utmost interest. To date, several electronic transitions of high-spin dimers and trimers have exclusively been measured in He droplets [3,6,7,18], where spin has also been a handle to initiate simple unimolecular reactions [6,18].

Recently, we measured the spin relaxation of alkali atoms and dimers on He droplets within a magnetic field, and demonstrated the possibility to create a net spin orientation and to optically address Zeeman substates [19]. In triplet dimers, a rich physics emerges from the combination of spin-orbit coupling and dopant-droplet interaction [20], further enriched in quartet trimers by the Jahn-Teller effect [21].

To date, no one has attempted a systematic investigation of quartet alkali trimers, perhaps deterred by the spectral congestion expected for the heavier trimers, and by the difficulty of a reliable assignment. In this Letter, we approach these two aspects with a combination of mass-selected beam depletion (MSBD) spectroscopy and double-resonance (DR) spectroscopy, backed by complete active space self-consistent field (CASSCF) *ab initio* calculations of the electronic structure of K_xRb_{3-x}, $x = 0 \ldots 3$, quartet trimers. We find a common level pattern, which will be interpreted in terms of a shell structure. The equilibrium structure is rigorously an equilateral triangle (A_2' state, $\mathcal{D}_{3h}$ symmetry) for K_3 and Rb_3, slightly distorted to an isosceles triangle (B_2 state, $\mathcal{C}_{2v}$ symmetry) for K_2Rb and KRb_2. To emphasize the common level pattern, in the text we identify all states with their $\mathcal{D}_{3h}$ labels, which correlate with $\mathcal{C}_{2v}$ as follows: $A_1' \rightarrow A_1$, $A_2' \rightarrow B_2$, $E' \rightarrow (A_1 + B_2)$, $A_1'' \rightarrow A_2$, $A_2'' \rightarrow B_1$, $E'' \rightarrow (A_2 + B_1)$.

The experimental setup has been described in detail elsewhere [22,23]. In brief, He droplets are produced via supersonic expansion in vacuum of He gas through a cold nozzle (diameter 5 μm, $T = 14$ K, stagnation pressure 60 bar, for an average size of $\bar{N} = 10^4$ atoms). The droplet beam is doped in two sequential pickup cells loaded with K and Rb metal, respectively, and separately heated. The cell temperature determines the statistical distribution of dopant atoms per droplet [24,25], and thus the spectra that are observed and their intensity. In the experiment described here, the doped droplet beam crosses two laser interaction zones, which we call the depletion zone and probe zone, respectively; the latter is fitted with a laser-induced-fluorescence (LIF) detector. Further downstream, the beam crosses a surface ionization detector (Langmuir-Taylor detector, LT) [26], hitting the ionizing rhenium ribbon at grazing incidence; most of the beam proceeds unhindered into a quadrupole mass spectrometer (QMS)

operating in counting mode. The lasers used are listed in Ref. [27].

LIF spectra were measured at a set of different pickup cell temperatures, as suitable for the target trimer. Of course, not all droplets are doped with the desired number of atoms, and the spectra of K [4], Rb [28], or their dimers [22] may appear. Up to now, the lower-lying transitions of dimers and homonuclear trimers have been addressed, and the occurrence of overlapping spectra has been rare. This is not so in the present investigation where a multitude of complexes is formed. When sufficient, these are identified via the unfolding of LIF signal versus vapor density inside the pickup cell (growth analysis) [23]. Beyond this, particularly for mixed trimers, we use two spectroscopic schemes relying on desorption of the dopants from their host droplet upon excitation [29].

The first scheme is a two-color V-type double-resonance measurement: The tagging laser crosses the beam in the depletion zone, where it excites a known transition, thus desorbing the target species. The second laser crosses in the probe zone, where the intensity of the LIF signal from the unknown transition is affected by the tagging laser only if the two transitions share the same ground state. The second scheme is based on mass-selective beam depletion: the ion signal from the QMS, set at the mass of the candidate species, is monitored as a laser is scanned across the transition. Again, a depletion signal is observed if the assignment is correct. The first scheme is more sensitive but relies on an accessible, known transition of the candidate species. The second is more flexible, but has a poorer signal.

With Rb only, we observe, in the spectral range of the Ti:Al_2O_3 laser, two new bands extending from 11 500 to 12 000 cm^{-1} (Figs. 1 and 2) and from 14 000 to 14 250 cm^{-1} (Fig. 2), which, based on signal growth analysis, we assign to the $2^4E' \leftarrow 1^4A_2'$ and $1^4A_1'' \leftarrow 1^4A_2'$ trimer transitions. With K only, we observe the known $2^4E' \leftarrow 1^4A_2'$ trimer transition [18].

With K and Rb simultaneously, we observe a complex LIF spectrum (Fig. 1, top panel). We decompose it by MSBD into four contributions: two from the above $2^4E' \leftarrow 1^4A_2'$ bands of K_3, Rb_3, and two new ones from the corresponding bands of K_2Rb, KRb_2. Traces in the bottom panel show MSBD signals for the most abundant isotopologues: at ion mass 163 (K_2Rb^+) and 209 (KRb_2^+). A scan at mass 255 (Rb_3^+) proves the method to work reliably, as LIF and MSBD spectra have exactly the same shape. Unexpectedly, the signal at mass 117 (K_3^+) was unstable and no useful MSBD spectrum could be recorded. As a further check, we verify that a weighted sum of the four trimers' spectra fully accounts for the profile of a typical LIF spectrum (Fig. 1, top panel. Also see Ref. [30]).

Four unstructured peaks, each from a different molecule, appear in the spectral range between 14 000 and 15 000 cm^{-1} (Fig. 2). The first, in order of increasing photon energy, belongs to Rb_3 (see above). The fourth

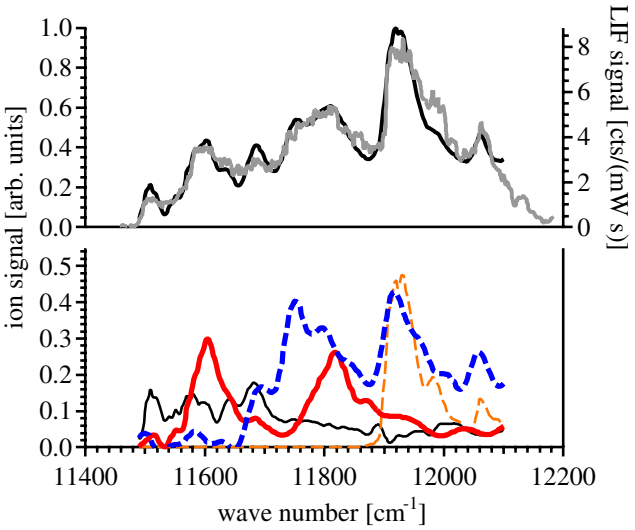

FIG. 1 (color online). Bottom panel: MSBD electronic-excitation spectra of K_xRb_{3-x} trimers, weighted to best fit the LIF spectrum above. Thick solid (red) line, KRb_2; thick dashed (blue) line, K_2Rb; thin solid (black) line, Rb_3; thin dashed (orange) line, K_3, LT beam-depletion spectrum. Top panel: Comparison between a typical LIF spectrum (gray line) and the sum of the individual depletion spectra (black line).

appears upon the presence of K; DR with the tagging laser set at 11 920 cm^{-1} (K_3) results in a 70% decrease of LIF, whereas tagging at 13 900 cm^{-1} (K_2) produces no effect.

The second and third peaks come from heteronuclear molecules. No dimer transitions are expected, according to potential energy curves [31]. Because of poor signal-to-noise ratio, no growth analysis was performed; we had previously observed, however, that an increase in Rb density in the pickup cell shifts the relative strength towards the second band, which is thus assigned to KRb_2. The third

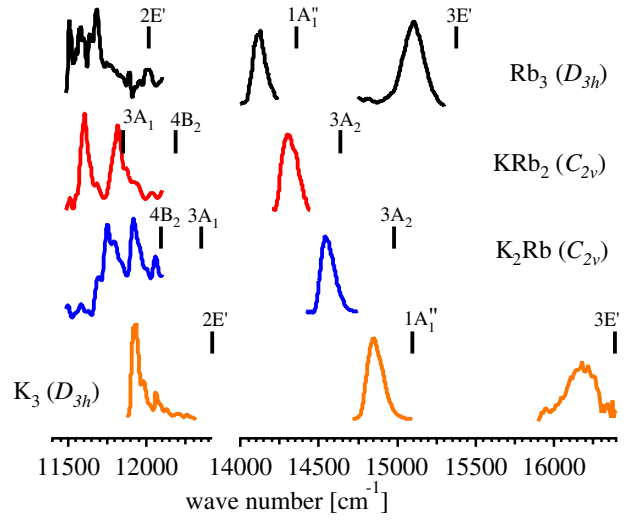

FIG. 2 (color online). Survey of the electronic-excitation bands of homo- and heteronuclear K_xRb_{3-x} trimers. Vertical lines mark the position of the *ab initio* transition energies (all quartet states).

band is assigned to K_2Rb: DR with the tagging laser tuned at 11 944 cm^{-1}, where the $2^4E' \leftarrow 1^4A_2'$ band of K_2Rb is strong, and that of KRb_2 weak, indeed shows $\approx 30\%$ depletion. The pattern of these four peaks suggests a similar electronic configuration of the participating states; we assign them to the $1^4A_1'' \leftarrow 1^4A_2'$ band.

Based on double resonance with $1^4A_1'' \leftarrow 1^4A_2'$, a new band of Rb_3 at $\approx$15 000 cm^{-1} is assigned to the $3^4E' \leftarrow 1^4A_2'$ transition. This band had already been observed in LIF excitation spectroscopy of Rb-doped helium droplets [32]. Dispersed-fluorescence spectra had shown emission from the $1^1\Pi_u \rightarrow 1^1\Sigma_g^+$ transition of free Rb_2, consistent with the excitation energy, but inconsistent with the concurrent emission from free Rb atoms: dissociation of Rb_2 from the $1^1\Pi_u$ state into any excited-atom channel is energetically forbidden. DR reveals that the excitation spectrum consists, in fact, of two transitions and allows their separation. The tagging laser is set to excite the Rb_3 band at 14 100 cm^{-1}, the probe laser is scanned twice, with and without the tagging laser, and LIF spectra are recorded. The difference signal (shown in Fig. 2) represents then a quartet Rb_3 spectrum, which accounts for the free-atom emission, while the unaffected portion (not shown) matches the Franck-Condon envelope of the $Rb_2\,1^1\Pi_u \leftarrow 1^1\Sigma_g^+$ transition (calculated using potentials from Ref. [33]). Likewise, with the $2^4E' \leftarrow 1^4A_2'$ transition of K_3 as a tag, we assign a similar structure at $\approx$16 200 cm^{-1} to a mixture of the $1^1\Pi_u \leftarrow 1^1\Sigma_g^+$ band of K_2 (potentials from Ref. [34]) and the $3^4E' \leftarrow 1^4A_2'$ band of K_3 (Fig. 2).

The range between 15 000 and 16 000 cm^{-1} is very congested (three dimer transitions also fall here), so we are unable to recognize and separate mixed trimers spectra. We also do not see (either in the experiment or in the calculations) the band previously observed at $\approx$12 800 cm^{-1} and tentatively assigned to the $1^4A_1'' \leftarrow 1^4A_2'$ transition of K_3 [18]. Because it does not fit the regular pattern we uncovered, we believe it must originate from some other oligomer.

Assignment of all the trimer transitions is based on *ab initio* calculations, performed with MOLPRO [35]. Details will be published separately; in brief, we use relativistic small-core effective-core potential basis sets of the Stuttgart/Cologne group [36]. We first optimize the geometry of the electronic ground state for all trimers at the RCCSD(T) level of theory (restricted coupled cluster calculations with single, double, and noniterative triple excitation). In agreement with Ref. [8], K_3 and Rb_3 are equilateral triangles with bond length and binding energy 5.06 Å, 1260 cm^{-1}, and 5.52 Å, 929 cm^{-1}, respectively. K_2Rb and KRb_2 are isosceles triangles with bond lengths 5.26 and 5.29 Å, angles 57.61° and 62.19°, and binding energies 1159 and 1049 cm^{-1}, respectively.

We calculate the vertical excitation energy at the global minimum geometry for the eight lowest optically active electronic transitions using the state-averaged CASSCF method of Werner and Knowles [37,38], with three electrons in the active space; because of restrictions in the computer code, all calculations are done in $\mathcal{C}_{2v}$ symmetry. At large internuclear separations, our calculations deviate from the experimental asymptotic (=atomic) excitation energies [39]. We enforce consistency by *ad hoc* shifts of the calculated states: +1500 and +1730 cm^{-1} for those correlating, respectively, to excited K and excited Rb; this gives the level pattern shown in Fig. 2. The splitting of the $2E'$ manifold for K_2Rb and KRb_2, due to the lower molecular symmetry, is clearly visible in the experimental spectra and is well reproduced by the calculations. The complicated structure of the same band in Rb_3 is due to the Jahn-Teller distortion with strong spin-orbit coupling, and will be analyzed separately [21].

The level structure underlying the observed spectra can be clarified in terms of delocalized orbitals, which reveal the existence of a shell structure. As often observed for single-particle states in quantum dots [9], the canonical orbitals from the *ab initio* calculations resemble harmonic-oscillator (HO) eigenfunctions. Because of the different strength of the potential in-plane and off-plane, we label orbitals, according to their nodal structure, with quantum numbers (n, ℓ, n_z) corresponding to a basis of two-dimensional HO eigenfunctions (Fock-Darwin orbitals [9]) in the molecular plane (r, θ) times one-dimensional HO eigenfunctions in the z direction; HO eigenvalues are $hc\tilde{\nu}_\rho(2n + |\ell| + 1) \equiv hc\tilde{\nu}_\rho(n_\rho + 1)$ and $hc\tilde{\nu}_z(n_z + 1/2)$. The energies ΔE of the lowest 13 orbitals, measured from (0, 0, 0), fit well to a 5-parameter formula with anharmonic and cross terms: $\Delta E/hc = n_\rho\tilde{\nu}_\rho + n_z\tilde{\nu}_z - x_\rho n_\rho^2\tilde{\nu}_\rho - x_z n_z^2\tilde{\nu}_z - x_{\rho z} n_\rho n_z\sqrt{\tilde{\nu}_\rho\tilde{\nu}_z}$. Because we only have $n_z = 0$ or 1, x_z is redundant and we set it to 0. The best fit parameters and rms of the residuals are reported in Table I. In a high-spin configuration, each orbital can accommodate only one of the three electrons (Pauli principle); in the ground state, the (0, 0, 0) orbital and the $(0, \pm 1, 0)$ pair are occupied. The observed bands correspond to excitations of one of the $(0, \pm 1, 0)$ electrons into $(0, \pm 2, 0)$ for $2E'$, and $(0, \pm 1, 1)$ for $1A_1''$. The $3E'$ band is a mix of shells arising from the degeneracy of $(1, \pm 1, 0)$, $(0, \pm 3, 0)$, and of the doubly excited state with both $(0, \pm 1, 0)$ electrons promoted to $(0, \pm 2, 0)$.

As the ground state corresponds to a complete $|\ell| = 1$ shell, we infer that the trimer should be more stable than the planar tetramer. This shell structure is the half-filled-orbitals analog of the celebrated observation in low-spin

TABLE I. Parameters of fit of orbital energies.

	$\tilde{\nu}_\rho$ (cm^{-1})	$\tilde{\nu}_z$ (cm^{-1})	x_ρ	x_z	$x_{\rho z}$	Res. rms (cm^{-1})
K_3	14 963	19 589	0.1237	0	0.3571	930
K_2Rb	14 269	18 747	0.1201	0	0.3353	1100
KRb_2	13 975	18 104	0.1161	0	0.2963	1210
Rb_3	13 312	17 329	0.1136	0	0.2754	1070

Na clusters [40]; it is remarkable that it occurs for high spins too, already at such a small number of atoms.

In summary, we measured the excitation spectra of all possible quartet-state homo- and heteronuclear trimers of K and Rb (K_xRb_{3-x}, $x = 0 \ldots 3$) in the spectral range from 10 600 to 17 400 cm^{-1}; we have separated and assigned them with a combination of pickup statistics, mass-selected beam depletion, and double-resonance spectroscopy. A regular pattern of bands common to all these trimers is observed, shifting to progressively lower photon energies across the series K_3, K_2Rb, KRb_2, Rb_3. Our high-level *ab initio* calculations of the corresponding excitation energies agree well with experimental data; the obtained electronic structure is interpreted in terms of harmonic-oscillator orbitals and indicates that a shell model is applicable to these high-spin adducts. The experimental method can be extended to any desired alkali-metal trimer and almost certainly will remain applicable to larger clusters, where the shell model will be of great help to assign and interpret the measured spectra.

Beyond the scope of this Letter, Rb_3 turns out to be a model system for the study of Jahn-Teller distortion combined with strong spin-orbit coupling. Also, our calculations yield the first ground-state potentials of mixed trimers, which are of importance for the investigation of cold atom-molecule collisions, and, more generally, of the interaction between spin-polarized alkali atoms.

We thank Pavel Soldán for advice on *ab initio* calculations. This research is supported by the Austrian Science Fund (FWF, Grant No. P18053-N02), and the European Research and Training Network (Contract No. HPRN-CT-2002-00290).

*Corresponding author.
wolfgang.ernst@tugraz.at

[1] Special issue on Helium Nanodroplets: A Novel Medium for Chemistry and Physics [J. Chem. Phys. **115** (2001)].
[2] M. Hartmann, R. E. Miller, J. P. Toennies, and A. Vilesov, Phys. Rev. Lett. **75**, 1566 (1995).
[3] J. Higgins *et al.*, J. Phys. Chem. A **102**, 4952 (1998).
[4] F. Stienkemeier *et al.*, Z. Phys. D **38**, 253 (1996).
[5] F. Ancilotto *et al.*, Z. Phys. B **98**, 323 (1995).
[6] J. Higgins *et al.*, Science **273**, 629 (1996).
[7] J. Higgins, W. E. Ernst, C. Callegari, J. Reho, K. K. Lehmann, G. Scoles, and M. Gutowski, Phys. Rev. Lett. **77**, 4532 (1996).
[8] P. Soldán, M. T. Cvitas, and J. M. Hutson, Phys. Rev. A **67**, 054702 (2003).
[9] S. M. Reimann and M. Manninen, Rev. Mod. Phys. **74**, 1283 (2002), and references therein.
[10] J. Herbig *et al.*, Science **301**, 1510 (2003).
[11] M. W. Zwierlein, C. A. Stan, C. H. Schunck, S. M. F. Raupach, S. Gupta, Z. Hadzibabic, and W. Ketterle, Phys. Rev. Lett. **91**, 250401 (2003).
[12] A. Simoni, F. Ferlaino, G. Roati, G. Modugno, and M. Inguscio, Phys. Rev. Lett. **90**, 163202 (2003).
[13] J. M. Hutson and P. Soldán, Int. Rev. Phys. Chem. **26**, 1 (2007).
[14] T. Köhler, K. Góral, and P. S. Julienne, Rev. Mod. Phys. **78**, 1311 (2006).
[15] J. M. Hutson and P. Soldán, Int. Rev. Phys. Chem. **25**, 497 (2006).
[16] T. Kraemer *et al.*, Nature (London) **440**, 315 (2006).
[17] E. Braaten and H. W. Hammer, Ann. Phys. (N.Y.) **322**, 120 (2007).
[18] J. H. Reho *et al.*, J. Chem. Phys. **115**, 10265 (2001).
[19] J. Nagl, G. Auböck, C. Callegari, and W. E. Ernst, Phys. Rev. Lett. **98**, 075301 (2007).
[20] G. Auböck *et al.*, J. Phys. Chem. A **111**, 7404 (2007).
[21] G. Auböck *et al.* (unpublished).
[22] O. Allard *et al.*, J. Phys. B **39**, S1169 (2006).
[23] J. Nagl *et al.*, J. Phys. Chem. A **111**, 12386 (2007).
[24] M. Hartmann *et al.*, J. Chem. Phys. **110**, 5109 (1999).
[25] S. Vongehr and V. V. Kresin, J. Chem. Phys. **119**, 11124 (2003).
[26] F. Stienkemeier, M. Wewer, F. Meier, and H. Lutz, Rev. Sci. Instrum. **71**, 3480 (2000).
[27] All lasers from Coherent, Inc. The pump laser is an Innova 200, power stabilized at 21 W, multiline visible. The tunable lasers, all multimode, are an 899-01 Ti:Al_2O_3 ring laser with mid- and shortwave optics, a 599 linear dye laser operating on DCM special, and a 699 ring dye laser operating on Rhodamine 6G.
[28] F. R. Brühl *et al.*, J. Chem. Phys. **115**, 10220 (2001).
[29] C. Callegari *et al.*, J. Phys. Chem. A **102**, 95 (1998).
[30] The LIF spectrum was taken in an earlier experimental run at slightly different conditions. Lacking an MSBD spectrum for the K_3 contribution, we use instead an older LT beam depletion spectrum.
[31] S. Rousseau, A. R. Allouche, and M. Aubert-Frécon, J. Mol. Spectrosc. **203**, 235 (2000).
[32] F. R. Brühl *et al.*, J. Chem. Phys. **115**, 10275 (2001).
[33] S. Park *et al.*, J. Mol. Spectrosc. **207**, 129 (2001).
[34] S. Magnier *et al.*, J. Chem. Phys. **121**, 1771 (2004).
[35] H.-J. Werner *et al.*, MOLPRO, version 2006.1, a package of *ab initio* programs (2006); see http://www.molpro.net.
[36] I. S. Lim *et al.*, J. Chem. Phys. **122**, 104103 (2005); http://www.theochem.uni-stuttgart.de/pseudopotentials/.
[37] H.-J. Werner and P. J. Knowles, J. Chem. Phys. **82**, 5053 (1985).
[38] P. J. Knowles and H.-J. Werner, Chem. Phys. Lett. **115**, 259 (1985).
[39] Y. Ralchenko *et al.*, NIST Atomic Spectra Database version 3.1.2 (2007); http://physics.nist.gov/asd3.
[40] W. D. Knight *et al.*, Phys. Rev. Lett. **52**, 2141 (1984).